

Mitigating Behavioral Hallucination in Multimodal Large Language Models for Sequential Images

Liangliang You^{*,1}, Junchi Yao^{*,1,3}, Shu Yang^{1,2}, Guimin Hu⁴, Lijie Hu^{†,1,2}, Di Wang^{†,1,2}

¹Provable Responsible AI and Data Analytics (PRADA) Lab

²King Abdullah University of Science and Technology

³University of Electronic Science and Technology of China ⁴University of Copenhagen

Abstract

While multimodal large language models excel at various tasks, they still suffer from hallucinations, which limit their reliability and scalability for broader domain applications. To address this issue, recent research mainly focuses on objective hallucination. However, for sequential images, besides objective hallucination, there is also behavioral hallucination, which is less studied. This work aims to fill in the gap. We first reveal that behavioral hallucinations mainly arise from two key factors: prior-driven bias and the snowball effect. Based on these observations, we introduce SHE (Sequence Hallucination Eradication), a lightweight, two-stage framework that (1) detects hallucinations via visual-textual alignment check using our proposed adaptive temporal window and (2) mitigates them via orthogonal projection onto the joint embedding space. We also propose a new metric (BEACH) to quantify behavioral hallucination severity. Empirical results on standard benchmarks demonstrate that SHE reduces behavioral hallucination by over 10% on BEACH while maintaining descriptive accuracy.

1 Introduction

Large language models (LLMs) have demonstrated powerful vision-language understanding and generation capabilities across various domains (Su et al., 2023; Yang et al., 2024a; Xu et al., 2023; Zhang et al., 2025; Yang et al., 2025; Cheng et al., 2025b; Hu et al., 2024). Recently, multimodal large language models (MLLMs), such as GPT-4V (Yang et al., 2023) and Qwen2-vl (Wang et al., 2024b), have been developed to extend to the visual modality. In particular, they achieve outstanding performance on tasks such as visual question answering (Ye et al., 2024), visual reasoning (Liu et al., 2024), video summarization (Hua

et al., 2025), and image captioning (Chen et al., 2024a). Despite their remarkable successes, these models still suffer from inherent limitations that lead to hallucinations, i.e., generating text that is semantically coherent but inconsistent with the visual content. Such errors raise critical reliability concerns, especially in sensitive domains like education, law, and medicine, where they can distort learning outcomes (Wang et al., 2024c; Li et al., 2023; Yin et al., 2023; Cheng et al., 2024; Ali et al., 2024; Zhang et al., 2024b; Cheng et al., 2025a; Yang et al., 2024b).

Recent research has made significant progress in addressing object hallucinations in MLLMs for single images through methods like knowledge grounding and representation learning (Yu et al., 2023; Jain et al., 2023; Ben-Kish et al., 2023; Zhao et al., 2023a). However, when the input is a sequence of images, besides object hallucinations, there are behavioral hallucinations, which are more challenging and less studied. In detail, object hallucination occurs when the model describes objects in images that are not actually there, making the output not match the real image. Behavioral hallucination is when a model makes up behaviors for objects in images that they should not be doing based on what’s actually shown (see Fig. 1 for an example). Unlike object hallucinations, these dynamic inconsistencies involve implausible actions or interactions between objects across temporal frames. To mitigate behavioral hallucinations, several approaches have been developed recently, such as Volcano (Lee et al., 2023) and Self-PEP (Wang et al., 2024d). However, these methods face limitations in either computational efficiency or dependency on external models; these would necessitate training external models or fine-tuning the original models, both of which greatly increase computational costs.

To address these gaps, we propose SHE (Sequence **H**allucination **E**radication), a novel

*Equal Contribution.

†Corresponding Author.

framework that detects and mitigates behavior hallucinations through latent representations. To motivate our method, we first reveal and analyze the prior-driven and snowball effects on generating behavioral hallucinations. Generally speaking, prior-driven mechanisms in MLLMs cause hallucinations by making the model rely too much on its existing biases from training, which skews its interpretation of inputs and leads to outputs that do not match reality. The snowball effect occurs when a single incorrect action prediction becomes the anchor that the model folds back into its context, triggering a cascading accumulation of additional related hallucinated behaviors.

Based on our analysis, SHE involves hallucination detection and mitigation stages. We detect hallucinations by checking how well patches of images match the text they generate. To further leverage the snowball effect, we propose an adaptive temporal windowing for the hallucination detection. Then, SHE involves using contextual embeddings to spot inconsistencies and then applying orthogonal projection in the vision embedding space to eliminate the hallucinated elements. By maintaining the consistency between visual and textual information without needing additional training, it enhances the reliability of MLLMs.

Compared to other methods, SHE shows superior performance across multiple evaluation metrics. Specifically, we propose an evaluation metric, namely BEACH, to better assess behavioral hallucinations, and show SHE achieves a 10% reduction in BEACH. These results confirm the effectiveness and practicality of our approach, offering a novel solution to the behavior hallucination problem in MLLMs for sequential images. Our contributions are threefold:

1. We provide comprehensive studies on the causes of behavior hallucinations and identify two key factors: the prior-driven effect and the snowball effect. We also analyze the correlation and difference between the influence of these two causes.
2. Based on our analysis, we propose SHE, a two-stage framework for addressing MLLM behavior hallucinations. SHE first detects behavior hallucinations using embeddings of our proposed adaptive temporal window, and then corrects them via projecting representations without extra training.
3. Our work addresses a research gap on behavioral hallucinations, with experiments showing that our method’s relief effectiveness surpasses baseline approaches. The results also demonstrate that SHE can effectively manage behavioral hallucinations while maintaining descriptive accuracy.

2 Related Work

Research on hallucination mitigation in multi-modal models spans four axes, i.e., data-level methods (Llava-1.5’s negative instruction tuning (Liu et al., 2023), caption rewriting (Wang et al., 2023)), model-centric enhancements (InternVL’s high-resolution grounding (Chen et al., 2023), HACL’s contrastive alignment (Zhao et al., 2023b)), dataset calibration via Hallucinator’s (Yu et al., 2023) cleaned instructions and counterfactual visual instructions to expand dataset diversity, and caption refinement with ReCaption’s rewritten in existing datasets to produce high-quality image–caption pairs (Xing et al., 2024).

Training innovations include RLHF-based methods like ViGoR (Yan et al., 2024) and frameworks such as MOCHA (Ben-Kish et al., 2023), which use dense rewards to align captions with human preferences and boost accuracy. Other RL approaches (HA-DPO (Zhao et al., 2023a), RLHF techniques (Sun et al., 2023)) prioritize factual responses to curb hallucinations. At inference, decoding strategies VCD (Leng et al., 2024), HALC (Chen et al., 2024b), IBD (Zhu et al., 2024), and guided methods like GCD (Deng et al., 2024) dynamically anchor generation to visual input, ensuring consistency. However, these techniques primarily target static object hallucinations through frame-wise processing, neglecting temporal dynamics in sequential inputs due to two gaps: (1) lack of inter-frame dependency modeling for error propagation control, and (2) reliance on multi-stage pipelines incurring prohibitive latency (e.g., Woodpecker (Yin et al., 2024) five-step correction). Thus, this prompts video-focused solutions to attempt temporal modeling, such as Volcano (Lee et al., 2023), VISTA-LLAMA (Ma et al., 2023), MERLIM (Villa et al., 2023).

Our research focuses on temporal hallucinations in image sequences, which are markedly distinct from existing methods. Most traditional approaches, such as LRV-Instruction, InternVL,

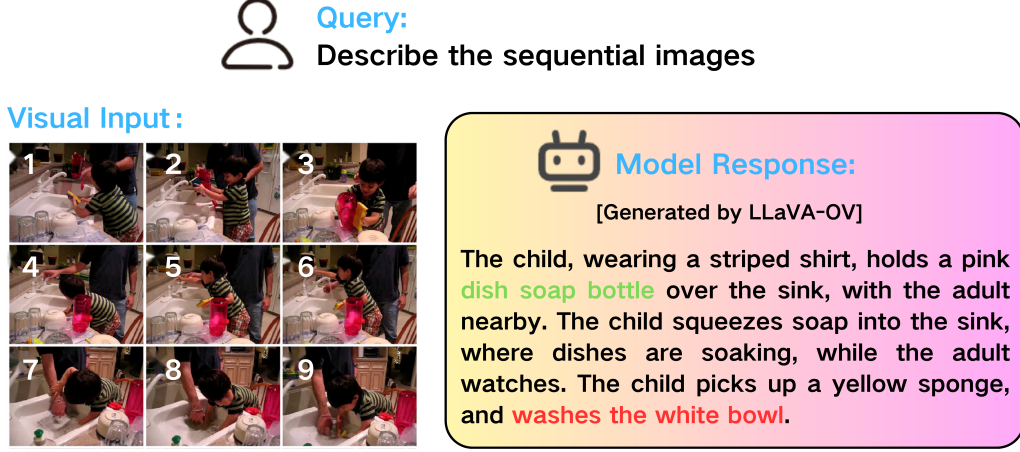


Figure 1: **Behavior hallucinations** indicate that the model generated behaviors not present in the image. There is no washing of a white bowl in the image; the bowl is simply placed on the table. **Object hallucinations** indicate that the output contains objects that are wrong or do not exist.

and VCD, concentrate on static object hallucinations by processing frames independently and thus overlook inter-frame dependencies, temporal dynamics, and effective use of visual context. Although recent video-oriented methods like Volcano and VISTA-LLAMA incorporate temporal information, they rely on reactive corrections and do not address the root causes of hallucinations.

3 Why MLLMs Generate Hallucinations?

Before detailing our proposed method, we first examine why MLLMs generate behavior hallucinations. Specifically, we identify two causes: the prior-driven effect and the snowball effect. Generally, the prior-driven effect induces hallucinations by causing the model to rely excessively on its pre-existing biases, which skews its interpretation of inputs and leads to outputs that do not match reality. The snowball effect in hallucinations occurs when a single incorrect action prediction becomes the anchor that the model folds back into its context, triggering a cascading accumulation of additional related hallucinated behaviors. We discuss these effects in the following subsections.

3.1 Prior-Driven Effects

To study the prior-driven effect on hallucinations, we examine how hallucinated behaviors are contextually linked to non-hallucinatory behaviors or hallucinatory objects, thereby revealing the model’s prior bias in generating related hallucinations. We quantify this alignment using the co-occurrence score, which measures the strength

of association between two elements by capturing how frequently they appear together within the same context (Kang and Choi, 2023). Intuitively, a high co-occurrence score between the generated response and the input image indicates that the model filled in missing or ambiguous visual details based on learned textual associations instead of relying on truly observed objects or behaviors. Thus, by measuring how often hallucinatory behaviors co-occur with specific objects or other behaviors, we directly capture the magnitude of the model’s prior-driven bias.

However, currently there are no metrics that are tailored for evaluating co-occurrence either between behaviors themselves or between behaviors and objects. To address this gap, we propose two novel metrics: one quantifies behavior-to-hallucinated behavior co-occurrence we call it **Co-Occurrence Score (Behavior-to-Hallucination Behavior) CoS(BH)**, and another measures hallucinated behavior-to-object co-occurrence we call it **Co-Occurrence Score (Hallucination Behavior-to-Object) CoS(BO)**. For the hallucinated and descriptive caption c generated by an MLLM for a set of sequence images, we define its CoS(BH) and CoS(BO) as the following. A larger value generally means more frequent hallucinations.

$$\text{CoS}_c(\text{BH}) = \sum_{i=1}^{n_h} \sum_{j=1}^{n_r} \frac{|C(b_{c,i}) \cap C(b_{c,j})|}{|C(b_{c,i})| + |C(b_{c,j})|},$$

where $b_{c,i}$ is the i -th hallucinatory behavior and $b_{c,j}$ is the j -th real behavior in caption c , $C(b_{c,i})$ is the set of all captions mentioning behavior $b_{c,i}$, n_h is the number of hallucinatory behaviors, and n_r

is the number of real behaviors. Generally speaking, $\text{CoS}_c(\text{BH})$ measures how often the hallucinated behaviors co-occur with non-hallucinated ones. See Fig. 2a for an example.

$$\text{CoS}_c(\text{BO}) = \sum_{i=1}^{n_h} \sum_{j=1}^m \frac{|C(b_{c,i}) \cap C(o_{c,j})|}{|C(b_{c,i})| + |C(o_{c,j})|},$$

where $o_{c,j}$ is the j -th hallucinatory object in caption c , $O(o_{c,j})$ is the set of all captions mentioning object $o_{c,j}$, and m is the number of hallucinatory objects in the object set. Unlike $\text{CoS}_c(\text{BH})$, $\text{CoS}_c(\text{BO})$ checks how well the model links behaviors to hallucinatory objects in a logical way that matches the context. See Figure 2b for an example.

For comparison, we also define corresponding scores for captions of the same image sequence that contain no hallucinatory behaviors. We sample n_h non-hallucinatory behaviors to match the hallucination group and let n_r and m be the same as before.

In our experiment, we consider Llava-OneVison (Li et al., 2024a) as the MLLM and the Mementos (Wang et al., 2024c) dataset. We start by using Llava-OneVision to generate captions for each image sequence in the dataset.

Results Analysis. Prior-driven effects indicate that MLLMs are sometimes driven by or influenced by their prior knowledge rather than carefully checking what is actually in the images. To quantify such prior bias, we use $\text{CoS}(\text{BH})$ and $\text{CoS}(\text{BO})$ to measure the extent to which the model’s hallucinations reflect learned associations.

In Figure 3a, captions containing behavioral hallucinations exhibit a pronounced bias: non-hallucinated captions mostly score between 0.05 and 0.15 while hallucinated ones are beyond 0.4. Moreover, Figure 3b, shows that the scores of non-hallucinated captions concentrate between 0.1 and 0.2 while hallucinated ones are more divergent. These patterns arise from the model’s reliance on prior knowledge acquired during training. During training, the model learns associations between behaviors, objects, and textual descriptions, which form its prior knowledge. When encountering unseen inputs without sufficient visual evidence, the model often defaults to these learned associations, leading to hallucinated behaviors. For example, if the model frequently associates a behavior with a specific object during training, it is more likely

to hallucinate that behavior when the object is present. Moreover, the model’s hallucinations also reflect learned object–behavior relationships from the training data.

Next, we demonstrate prior bias through attention distribution, which refers to the allocation of the model’s focus between different input modalities, such as text and visual tokens. Attention analysis in Appendix Fig. 7 shows that 87% of the model’s attention is allocated to text tokens, despite visual tokens comprising nearly 90% of the total tokens. This imbalance underscores the model’s reliance on prior knowledge and amplifies the prior-driven effects, thereby contributing to hallucinations.

3.2 Snowball Effects

To examine this effect, we use the Video-MME (Fu et al., 2024) dataset. After filtering out low-quality or incompletely annotated videos, we categorize the remaining samples by duration: short (<2 min), medium (2–10 min), and long (>10 min). For each category, we compute the behavior hallucination rate (BH) and object hallucination rate (OH) as the ratio of hallucinated responses to the total number of responses. Figure 4a shows a clear increase in hallucination rate with increasing video length, indicating a positive correlation between sequence duration and hallucination prevalence.

Next, we assess the effect of sampling density. For each category, we extract frames at 1, 2, and 3 fps and compute the behavior hallucination rate (BH) as the ratio of hallucinated responses to the total number of responses. Figure 4b shows that longer sequences and higher sampling rates lead to increased hallucination rates, reinforcing the observed correlation and motivating our subsequent controlled perturbation experiments.

To further explore the relationship between behavioral hallucinations and cumulative snowball effects, we perform stage-wise perturbations on each sequence. We divide each image sequence into ten equal segments s_i ($i = 1, \dots, 10$) and introduce either Gaussian blur ($\sigma = 1.5$) (Zhang et al., 2024a) or 20% random occlusion (Wu et al., 2024) to each segment. We then measure the change in behavior hallucination rate. Figure 4c shows that perturbing the first segment (the first 10% of frames) yields the largest increase in hallucinations, confirming that early errors disproportionately propagate and amplify through the se-

Prompt : Write a description for the given image sequence in a single paragraph, what is happening in this sequence?



MLLM : These shows a man is holding a microphone and making emotional jewelry with hands, he is delivering a passionate oration.

This is a non-hallucinatory behavior

This is a hallucinatory behavior (Co-Occurrence)

(a) An example of behavior-to-hallucination behavior co-occurrence.

Prompt : Write a description for the given image sequence in a single paragraph, what is happening in this sequence?



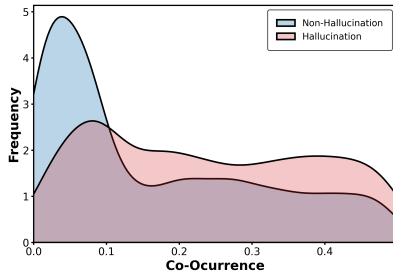
MLLM : In this sequence of images, we observe the man in the red hoodie draws Poker, while the man wearing glasses walks away. They're having a poker game

This is a hallucinatory object

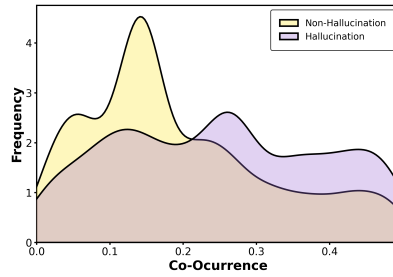
This is a hallucinatory behavior (Co-Occurrence)

(b) An example of hallucination behavior-to-object co-occurrence.

Figure 2: **(a)** The model correctly recognizes “making emotional jewelry” (highlighted in red), but then hallucinates by generating “holding a microphone.” **(b)** The model correctly identifies “Poker” (highlighted in blue), yet hallucinates by producing “have poker gaming.”



(a) $\text{CoS}_c(\text{BH})$



(b) $\text{CoS}_c(\text{BH})$

Figure 3: Distribution of $\text{CoS}_c(\text{BH})$ and $\text{CoS}_c(\text{BH})$ for hallucinatory and non-hallucinatory captions.

quence.

To summarize, our results show that hallucinations increase rapidly as the input sequence lengthens, especially for behavioral hallucinations. This trend occurs because the model processes each frame sequentially: an early mistake leads to more mistakes later. For objective hallucinations, errors are static—for example, the model might label a “chair” as a “table” in every frame. In contrast, behavioral hallucinations evolve over time: misrecognizing one action can trigger a cascade of unlikely behavior predictions that intensify throughout the sequence. Stage-specific perturbation experiments in Figure 4c further illustrate this effect, showing that disturbances in early frames have the greatest impact. Noise injected into the first 10% of frames accounts for 76.7% of all behavioral hallucination perturbations in the middle frames contribute 42%, and those in the final frames have negligible impact. These findings underscore the critical influence of initial processing stages: errors in the first few frames heavily bias subse-

quent predictions, especially for complex behavioral tasks.

4 SHE: Sequence Hallucination Eradication

In this section, we detail our methodology. SHE concurrently addresses both hallucination mechanisms: for prior-driven effects caused by knowledge-visual misalignment, we detect them by measuring similarity between visual features and textual captions; to handle snowball effects, we employ adaptive temporal windows. To mitigate these effects, we eliminate spurious associations via orthogonal projection in the joint embedding space, enforcing visually grounded reasoning while preserving linguistic coherence.

4.1 Detection

Visual-Textual Alignment Check. Motivated by the finding in Section 3.1 that visual tokens receive little attention—MLLMs focus less on visual evidence—we quantify semantic congruence

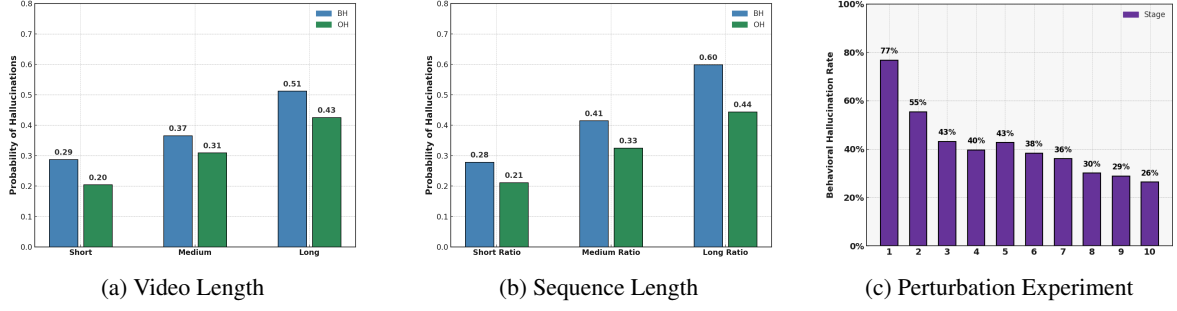


Figure 4: **(a)** Distribution of hallucination rates for behavioral hallucination (BH) and objective hallucination(OH) with different video lengths. **(b)** Distribution of hallucination rates for BH and OH for different lengths of the same videos. **(c)** Behavioral hallucination rates after perturbing frames at different stages.

between language captions and visual inputs. We measure the similarity between contextual embeddings and image patch embeddings to detect hallucinations. For each generated caption, we extract contextual embeddings of behavior tokens from intermediate layers and compute the global behavior representation e_{Beh} by averaging:

$$e_{Beh} = \frac{1}{n} \sum_{i=1}^n e_{l_T}(t_i),$$

where $\{t_1, t_2, \dots, t_n\}$ are the tokens for representing the behavior to be detected, and $e_{l_T}(t_i)$ denotes the embedding of token t_i at layer l_T (layer selection is discussed in the experimental part). For each frame in the image sequence, we divide the image into patches and extract embeddings $e_{l_I}(p_j)$ for each patch p_j .

We then compute the cosine similarity between the behavior embedding e_{Beh} and each patch's embedding $e_{l_I}(p_j)$ in every layer:

$$\text{Score}(p_j) = \max_{l_I \in \{1, 2, \dots, L\}} \cos(e_{Beh}, e_{l_I}(p_j)).$$

This score quantifies semantic consistency between image patches and the behavior in the spatio-temporal domain. For each frame f , we aggregate its patch scores to compute a frame-level match metric. We then aggregate these metrics across all frames—typically using the maximum patch score across all frames as the global confidence score:

$$\text{Confidence} = \max_{f \in \text{frames}, p_j \in f} \text{Score}(p_j).$$

Confidence scores reflect the degree to which a behavior is grounded in visual evidence. Behaviors with higher scores are regarded as non-hallucinated, while those with lower scores are considered likely to be hallucinated.

Adaptive Temporal Windowing. To mitigate the accumulation of hallucinations over time, we propose adaptive temporal windowing to address the snowball effect. Specifically, for each image patch p_j^t requiring correction, we aggregate features from adjacent frames, thereby enhancing the robustness of our method:

$$E_{\text{agg}}(p_j^t) = \{e_{l_I}(p_j^{t-\tau/2}), \dots, e_{l_I}(p_j^t), \dots, e_{l_I}(p_j^{t+\tau/2})\},$$

where τ , the temporal window radius determined by behavior complexity, is adaptively scaled by the entropy of e_{Beh} . This adaptive scaling ensures that embeddings with higher semantic uncertainty receive wider windows to capture additional spatio-temporal context and mitigate cascading hallucinations. Specifically, we define:

$$\tau = \lceil \gamma \cdot \text{Entropy}(e_{Beh}) \rceil.$$

4.2 Mitigation

The mitigation strategy directly addresses the causal chain identified in Section 3 through targeted interventions. Based on the finding that behavioral hallucinations stem from prior-driven object misalignments, we first perform object grounding by orthogonalizing visual features against hallucinated object embeddings, thereby eliminating the root cause of behavioral errors before they propagate temporally. For each hallucinated behavior $b_i \in B_{\text{hallu}}$ identified in the previous stage, we apply the following steps:

Step 1: Extracting Behavior Text Embeddings. We aggregate the intermediate text-encoder embeddings of the hallucinated behavior tokens and average them to form a compact semantic vector that captures the core meaning of the erroneous behavior. We then extract the intermediate layer embedding of behavior b_i using the text encoder: $\vec{e}_i = e_{l_T}(b_i)$.

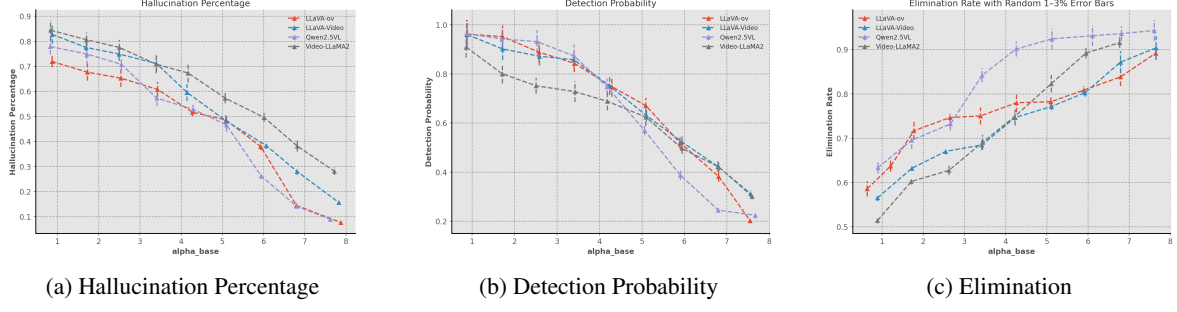


Figure 5: **(a)** The probability of hallucination occurrence across the four models. **(b)** The probability of hallucinations being detected. **(c)** The probability of successful hallucination elimination.

Step 2: Correcting Image Features. We orthogonally project each aggregated image-patch feature against the behavior embedding, removing the visual components that align with the hallucinated behavior. Specifically, we perform an orthogonal projection of the aggregated image feature $e_{\text{agg}}(p_j^t)$ along the direction of the behavior text embedding at layer l_T :

$$E_{\text{corrected}}(p_j^t) = \left\{ E - \alpha \cdot \frac{E \cdot \vec{e}_i}{\|\vec{e}_i\|_2^2} \cdot \vec{e}_i \mid E \in E_{\text{agg}}(p_j^t) \right\}.$$

To prevent excessive correction that could diminish genuine visual information, we limit the adjustment intensity via a correction strength coefficient α , which is dynamically scaled according to detection confidence:

$$\alpha = \alpha_{\text{base}} \cdot (1 - \text{Confidence}_{\text{max}}(p_j^t)).$$

Intuitively, a lower confidence score, which indicates a higher risk of hallucination, should result in a stronger correction.

Step 3: Feature Re-injection. We replace the original intermediate-layer visual features with their corrected versions, ensuring that subsequent predictions rely on de-biased, hallucination-corrected visual representations, i.e., we replace the original intermediate layer representation $e_{l_I}(p_j^t)$ with the corrected features $E_{\text{corrected}}(p_j^t)$.

5 Experiment

5.1 Experimental Setup

Datasets. We evaluate our approach on four widely used benchmarks: **Mementos** (Wang et al., 2024c) for sequential image captioning, **SSID** (Lastname, 2025) for video-based hallucination analysis, **VWP** (Hong et al., 2023), and **Visual Storytelling** (Huang et al., 2016). Details are in Appendix A.4.

Baselines. We compare our method with three state-of-the-art approaches: **DeCo** (Wang et al., 2024a) (dynamic correction decoding), **VCD** (Leng et al., 2024) (contrastive decoding), and **OPERA** (Huang et al., 2024) (over-trust penalty). Details are in Appendix A.6.

Models. Experiments are conducted with advanced open-source multimodal large language models, including LLaVA-ov (Li et al., 2024a), Qwen2.5-vl (Bai et al., 2025), LLaVA-Next-Video (Li et al., 2024b), and Video-LLaMA (Zhang et al., 2023).

Evaluation Metrics. We adopt mAP and CHAIR (Rohrbach et al., 2018) as primary evaluation metrics for hallucination mitigation, in line with prior work. Additionally, we introduce **BEACH** to assess behavioral hallucinations. Details are in Appendix A.5.

Implementation Details. In the experiments, for models based on the LLaVA architecture, we set the α_{base} to $[4, 5]$, and γ to $[0.4, 0.6]$. For models using the Qwen-VL architecture, the beta value was set to 0.45, α_{base} to $[4, 5]$, and γ to $[0.4, 0.6]$.

5.2 Experimental Results

Results in Table 1 demonstrate that the proposed method consistently improves hallucination suppression and behavior detection accuracy across four datasets and three model architectures. All evaluated models exhibit reductions in two BEACH metrics, accompanied by increases in mAP. Comparable but more modest improvements occur with LLaVA-ov and LLaVA-Video, reflecting their higher baseline hallucination propensity and more verbose narrative style. Qwen-2.5VL’s richer internal representations and succinct, to-the-point outputs naturally limit spurious details, making our correction mechanism especially effective; by contrast, the elaborated descriptions characteristic of the LLaVA variants in-

Table 1: Behavior Hallucination Evaluation Results.

Method	Qwen-2.5VL _{behavior}			LLaVA-ov _{behavior}			LLaVA-Video _{behavior}		
	BEACH_S ↓	BEACH_I ↓	mAP ↑	BEACH_S ↓	BEACH_I ↓	mAP ↑	BEACH_S ↓	BEACH_I ↓	mAP ↑
Momentos									
DECO	45.89	89.74	0.09	50.69	64.08	0.27	53.22	63.37	0.28
VCD	43.32	59.02	0.31	45.50	61.81	0.29	47.78	64.55	0.29
OPERA	38.88	57.71	0.30	53.94	69.13	0.25	56.68	67.12	0.27
Ours	35.91	55.33	0.31	42.33	59.49	0.33	46.92	58.41	0.33
SSID									
DECO	41.71	78.79	0.19	47.63	60.57	0.30	50.01	61.88	0.28
VCD	34.88	54.77	0.35	43.17	59.02	0.31	46.62	55.47	0.33
OPERA	37.10	60.82	0.29	50.39	65.72	0.29	52.91	67.99	0.27
Ours	33.91	53.56	0.35	40.26	57.82	0.32	41.83	53.11	0.34
Visual Storytelling									
DECO	36.65	65.81	0.26	46.47	68.74	0.26	48.79	71.68	0.23
VCD	37.34	68.42	0.21	41.71	58.77	0.30	43.80	59.52	0.32
OPERA	28.51	57.54	0.33	49.44	63.37	0.28	51.91	57.14	0.35
Ours	25.11	53.17	0.35	38.80	54.53	0.32	40.74	57.26	0.35
Visual VWP									
DECO	57.28	74.81	0.22	45.77	69.41	0.26	48.43	66.58	0.25
VCD	31.92	59.76	0.28	41.71	58.77	0.31	44.13	64.79	0.29
OPERA	31.06	62.94	0.25	49.44	60.73	0.28	52.30	57.38	0.31
Ours	27.43	56.39	0.31	37.80	52.59	0.34	40.17	54.11	0.35

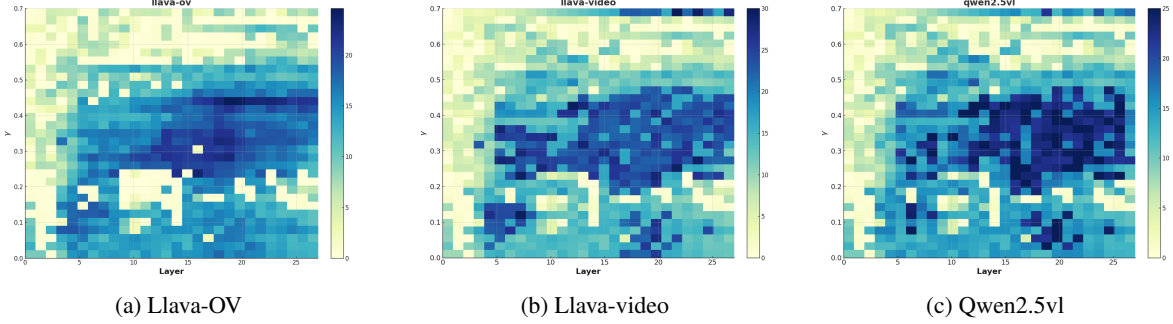


Figure 6: **(a)** Hallucination reduction across different layers and γ value in Llava-OV model. **(b)** Hallucination reduction across different layers and γ value in Llava-Video model. **(c)** Hallucination reduction across different layers and γ value in Qwen-2.5vl model.

Table 2: Object Hallucination on Momentos.

Method	Qwen-2.5VL _{object}			LLaVA-ov _{object}		
	CHAIR_S ↓	CHAIR_I ↓	mAP ↑	CHAIR_S ↓	CHAIR_I ↓	mAP ↑
DECO	62.68	93.21	0.07	61.14	57.33	0.43
VCD	29.38	38.75	0.64	57.79	55.30	0.44
OPERA	34.74	45.35	0.56	62.39	50.78	0.51
Ours	31.76	36.63	0.65	50.72	48.63	0.53

introduce additional opportunities for hallucination and thus require stronger adjustments to reach similar gains. Overall, these results confirm that our approach consistently achieves a favorable balance between hallucination mitigation and descriptive fidelity, with the degree of improvement closely tied to each model’s inherent capacity and output style.

Table 2 reports object hallucination metrics on the Momentos dataset. The performance gap between our approach and the baselines on two CHAIR metrics is minimal, demonstrating that the behavioral hallucination suppression achieved by

our method does not introduce additional object hallucinations.

5.3 Ablation Study

We conducted ablation studies on the correction strength α_{base} and the temporal window coefficient γ , comparing fixed and dynamic strategies. Our experiments reveal that both parameters play a crucial role in balancing hallucination mitigation and output utility. Specifically, moderate values of α_{base} and γ —in conjunction with edits applied to middle-to-late network layers—achieve the best trade-off between hallucination reduction and descriptive fidelity. Excessively large values for either parameter can degrade output informativeness or correction accuracy. Further details and comprehensive analysis of these ablation experiments are provided in Appendix A.7

6 Conclusion

This paper introduces SHE, a lightweight framework for mitigating behavioral hallucinations in multimodal large language models for sequential images. By analyzing the underlying causes, we reveal the roles of prior-driven bias and the snowball effect, and propose a two-stage solution with adaptive temporal window detection and orthogonal projection. Experiments on four benchmarks show that SHE effectively reduces behavioral hallucinations while preserving descriptive accuracy. The proposed BEACH metric also enables more precise evaluation of hallucination severity.

Limitation

Despite the effectiveness of SHE in reducing behavioral hallucinations on a range of sequential image benchmarks, several limitations remain to be addressed. First, the framework is specifically developed for sequential images, and its applicability to other modalities such as continuous video streams or complex audio-visual data has not yet been thoroughly validated. Furthermore, the detection and mitigation steps in SHE rely on threshold-based decisions and hyperparameters, which may require careful tuning for new models or tasks to maintain optimal performance. Another limitation is the assumption of access to intermediate representations within the multimodal model. While SHE does not require additional training or model fine-tuning, it still presumes that users can extract hidden layer embeddings, which may not be feasible for proprietary, closed-source, or highly abstracted systems. However, we believe future advances in model interpretability could alleviate this constraint. We also believe SHE still offers valuable insights for controlling hallucinations in sequential visual reasoning.

References

- Muhammad Asif Ali, Nawal Daftardar, Mutayyaba Waheed, Jianbin Qin, and Di Wang. 2024. Mqa-keal: Multi-hop question answering under knowledge editing for arabic language. *arXiv preprint arXiv:2409.12257*.
- Shuai Bai, Keqin Chen, Xuejing Liu, Jialin Wang, Wenbin Ge, Sibao Song, Kai Dang, Peng Wang, Shijie Wang, Jun Tang, and 1 others. 2025. Qwen2. 5-vl technical report. *arXiv preprint arXiv:2502.13923*.
- Assaf Ben-Kish, Moran Yanuka, Morris Alper, Raja Giryes, and Hadar Averbuch-Elor. 2023. Mocha: Multi-objective reinforcement mitigating caption hallucinations. *arXiv preprint arXiv:2312.03631*.
- Xiaohui Chen, Satya Narayan Shukla, Mahmoud Azab, Aashu Singh, Qifan Wang, David Yang, ShengYun Peng, Hanchao Yu, Shen Yan, Xuewen Zhang, and Baosheng He. 2024a. Compcap: Improving multimodal large language models with composite captions. *arXiv preprint arXiv:2412.05243*.
- Zhaorun Chen, Zhuokai Zhao, Hongyin Luo, Huaxiu Yao, Bo Li, and Jiawei Zhou. 2024b. Halc: Object hallucination reduction via adaptive focal-contrast decoding. *arXiv preprint arXiv:2403.00425*.
- Zhe Chen, Jiannan Wu, Wenhai Wang, Weijie Su, Guo Chen, Sen Xing, Zhong Muyan, Qinglong Zhang, Xizhou Zhu, Lewei Lu, and 1 others. 2023. Internvl: Scaling up vision foundation models and aligning for generic visual-linguistic tasks. *arXiv preprint arXiv:2312.14238*.
- Keyuan Cheng, Zijian Kan, Zhixian He, Zhuoran Zhang, Muhammad Asif Ali, Ke Xu, Lijie Hu, and Di Wang. 2025a. Compke: Complex question answering under knowledge editing. *arXiv preprint arXiv:2506.00829*.
- Keyuan Cheng, Gang Lin, Haoyang Fei, Lu Yu, Muhammad Asif Ali, Lijie Hu, Di Wang, and 1 others. 2024. Multi-hop question answering under temporal knowledge editing. *arXiv preprint arXiv:2404.00492*.
- Keyuan Cheng, Xudong Shen, Yihao Yang, Tengyue Wang, Yang Cao, Muhammad Asif Ali, Hanbin Wang, Lijie Hu, and Di Wang. 2025b. Codemenv: Benchmarking large language models on code migration. *arXiv preprint arXiv:2506.00894*.
- Ailin Deng, Zhirui Chen, and Bryan Hooi. 2024. Seeing is believing: Mitigating hallucination in large vision-language models via clip-guided decoding. *arXiv preprint arXiv:2402.15300*.
- Chaoyou Fu, Yuhao Dai, Yongdong Luo, Lei Li, Shuhuai Ren, Renrui Zhang, Zihan Wang, Chenyu Zhou, Yunhang Shen, Mengdan Zhang, Peixian Chen, Yanwei Li, Shaohui Lin, Sirui Zhao, Ke Li, Tong Xu, Xiwu Zheng, and Xing Sun. 2024. Video-mme: The first-ever comprehensive evaluation benchmark of multi-modal llms in video analysis. *arXiv preprint arXiv:2405.21075*.
- Xudong Hong, Asad Sayeed, Khushboo Mehra, Vera Demberg, and Bernt Schiele. 2023. [Visual writing prompts: Character-grounded story generation with curated image sequences](#). *arXiv preprint arXiv:2301.08571*. Accessed: 2025-05-15.
- Lijie Hu, Liang Liu, Shu Yang, Xin Chen, Zhen Tan, Muhammad Asif Ali, Mengdi Li, and Di Wang. 2024. Understanding reasoning in chain-of-thought from the hopfieldian view. *arXiv preprint arXiv:2410.03595*.

- Hang Hua, Yunlong Tang, Chenliang Xu, and Jiebo Luo. 2025. V2xum-llm: Cross-modal video summarization with temporal prompt instruction tuning. In *Proceedings of the AAAI Conference on Artificial Intelligence*, volume 39, pages 3599–3607.
- Qidong Huang, Xiaoyi Dong, Pan Zhang, Bin Wang, Conghui He, Jiaqi Wang, Dahua Lin, Weiming Zhang, and Nenghai Yu. 2024. Opera: Alleviating hallucination in multi-modal large language models via over-trust penalty and retrospection-allocation. In *Proceedings of the IEEE/CVF Conference on Computer Vision and Pattern Recognition*, pages 13418–13427.
- Ting-Hao Huang, Francis Ferraro, Nasrin Mostafazadeh, Ishan Misra, Aishwarya Agrawal, Jacob Devlin, Ross Girshick, Xiaodong He, Pushmeet Kohli, Dhruv Batra, C. Lawrence Zitnick, Devi Parikh, Lucy Vanderwende, Michel Galley, and Margaret Mitchell. 2016. [Visual storytelling](#). *arXiv preprint arXiv:1604.03968*. Accessed: 2025-05-15.
- Jitesh Jain, Jianwei Yang, and Humphrey Shi. 2023. Vcoder: Versatile vision encoders for multi-modal large language models. *arXiv preprint arXiv:2312.14233*.
- Cheongwoong Kang and Jaesik Choi. 2023. [Impact of co-occurrence on factual knowledge of large language models](#). *arXiv preprint arXiv:2310.08256*.
- Firstname Lastname. 2025. [Sequential vision to language as story: A storytelling dataset and benchmark](#). *IEEE Journals & Magazine*. Accessed: 2025-05-15.
- Seongyun Lee, Sue Hyun Park, Yongrae Jo, and Minjoon Seo. 2023. Volcano: mitigating multimodal hallucination through self-feedback guided revision. *arXiv preprint arXiv:2311.07362*.
- Sicong Leng, Hang Zhang, Guanzheng Chen, Xin Li, Shijian Lu, Chunyan Miao, and Lidong Bing. 2023. [Mitigating object hallucinations in large vision-language models through visual contrastive decoding](#). *arXiv preprint arXiv*, 2311.16922.
- Sicong Leng, Hang Zhang, Guanzheng Chen, Xin Li, Shijian Lu, Chunyan Miao, and Lidong Bing. 2024. Mitigating object hallucinations in large vision-language models through visual contrastive decoding. In *Proceedings of the IEEE/CVF Conference on Computer Vision and Pattern Recognition*, pages 13872–13882.
- Bo Li, Yuanhan Zhang, Dong Guo, Renrui Zhang, Feng Li, Hao Zhang, Kaichen Zhang, Peiyuan Zhang, Yanwei Li, Ziwei Liu, and 1 others. 2024a. Llava-onevision: Easy visual task transfer. *arXiv preprint arXiv:2408.03326*.
- Feng Li, Renrui Zhang, Hao Zhang, Yuanhan Zhang, Bo Li, Wei Li, Zejun Ma, and Chunyuan Li. 2024b. Llava-next-interleave: Tackling multi-image, video, and 3d in large multimodal models. *arXiv preprint arXiv:2407.07895*.
- Yifan Li, Yifan Du, Kun Zhou, Jinpeng Wang, Wayne Xin Zhao, and Ji-Rong Wen. 2023. Evaluating object hallucination in large vision-language models. *arXiv preprint arXiv:2305.10355*.
- Fuxiao Liu, Kevin Lin, Linjie Li, Jianfeng Wang, Yaser Yacoob, and Lijuan Wang. 2023. Mitigating hallucination in large multi-modal models via robust instruction tuning. *arXiv preprint arXiv:2306.14565*.
- Ziyu Liu, Zeyi Sun, Yuhang Zang, Wei Li, Pan Zhang, Xiaoyi Dong, Yuanjun Xiong, Dahua Lin, and Jiaqi Wang. 2024. Rar: Retrieving and ranking augmented mllms for visual recognition. *arXiv preprint arXiv:2403.13805*.
- Fan Ma, Xiaojie Jin, Heng Wang, Yuchen Xian, Jiashi Feng, and Yi Yang. 2023. [Vista-llama: Reliable video narrator via equal distance to visual tokens](#). *arXiv preprint arXiv:2312.08870*.
- Anna Rohrbach, Lisa Anne Hendricks, Kaylee Burns, Trevor Darrell, and Kate Saenko. 2018. Object hallucination in image captioning. *arXiv preprint arXiv:1809.02156*.
- Jinyan Su, Terry Yue Zhuo, Di Wang, and Preslav Nakov. 2023. Detectllm: Leveraging log rank information for zero-shot detection of machine-generated text. *arXiv preprint arXiv:2306.05540*.
- Zheng Sun, Shijun Shen, Sheng Cao, Hao Liu, Chong Li, Yi Shen, Chuang Gan, Li-Yi Gui, Yong-Xiang Wang, and Yi et al. Yang. 2023. Aligning large multimodal models with factually augmented rlhf. *arXiv preprint arXiv:2309.14525*.
- Andrés Villa, Juan Carlos León Alcázar, Alvaro Soto, and Bernard Ghanem. 2023. Behind the magic, merlim: Multi-modal evaluation benchmark for large image-language models. *arXiv preprint arXiv:2312.02219*.
- Chenxi Wang, Xiang Chen, Ningyu Zhang, Bozhong Tian, Haoming Xu, Shumin Deng, and Huajun Chen. 2024a. Mllm can see? dynamic correction decoding for hallucination mitigation. *arXiv preprint arXiv:2410.11779*.
- Lei Wang, Jiabang He, Shenshen Li, Ning Liu, and Ee-Peng Lim. 2023. [Mitigating fine-grained hallucination by fine-tuning large vision-language models with caption rewrites](#). *arXiv preprint arXiv:2312.01701*.
- Peng Wang, Shuai Bai, Sinan Tan, Shijie Wang, Zhihao Fan, Jinze Bai, Keqin Chen, Xuejing Liu, Jialin Wang, Wenbin Ge, and 1 others. 2024b. Qwen2-vl: Enhancing vision-language model’s perception of the world at any resolution. *arXiv preprint arXiv:2409.12191*.
- Xiyao Wang, Yuhang Zhou, Xiaoyu Liu, Hongjin Lu, Yuancheng Xu, Feihong He, Jaehong Yoon, Taixi Lu, Gedas Bertasius, Mohit Bansal, and 1 others. 2024c. Mementos: A comprehensive benchmark

- for multimodal large language model reasoning over image sequences. *arXiv preprint arXiv:2401.10529*.
- Yuxuan Wang, Yueqian Wang, Dongyan Zhao, Cihang Xie, and Zilong Zheng. 2024d. Videohalluciner: Evaluating intrinsic and extrinsic hallucinations in large video-language models. *arXiv preprint arXiv:2406.16338*.
- Xiyang Wu, Tianrui Guan, Dianqi Li, Shuaiyi Huang, Xiaoyu Liu, Xijun Wang, Ruiqi Xian, Abhinav Shrivastava, Furong Huang, Jordan Lee Boyd-Graber, Tianyi Zhou, and Dinesh Manocha. 2024. Autohallusion: Automatic generation of hallucination benchmarks for vision-language models. *arXiv preprint arXiv:2406.10900*.
- Shangyu Xing, Fei Zhao, Zhen Wu, Tuo An, Weihao Chen, Chunhui Li, Jianbing Zhang, and Xinyu Dai. 2024. Efuf: Efficient fine-grained unlearning framework for mitigating hallucinations in multimodal large language models. *arXiv preprint arXiv:2402.09801*.
- Xilie Xu, Keyi Kong, Ning Liu, Lizhen Cui, Di Wang, Jingfeng Zhang, and Mohan Kankanhalli. 2023. An llm can fool itself: A prompt-based adversarial attack. *arXiv preprint arXiv:2310.13345*.
- Siming Yan, Min Bai, Weifeng Chen, Xiong Zhou, Qixing Huang, and Li Erran Li. 2024. Vigor: Improving visual grounding of large vision language models with fine-grained reward modeling. *arXiv preprint arXiv:2402.06118*.
- Shu Yang, Muhammad Asif Ali, Lu Yu, Lijie Hu, and Di Wang. 2024a. Monal: Model autophagy analysis for modeling human-ai interactions. *arXiv preprint arXiv:2402.11271*.
- Shu Yang, Shenzhe Zhu, Ruoxuan Bao, Liang Liu, Yu Cheng, Lijie Hu, Mengdi Li, and Di Wang. 2024b. What makes your model a low-empathy or warmth person: Exploring the origins of personality in llms. *arXiv preprint arXiv:2410.10863*.
- Shu Yang, Shenzhe Zhu, Zeyu Wu, Keyu Wang, Junchi Yao, Junchao Wu, Lijie Hu, Mengdi Li, Derek F Wong, and Di Wang. 2025. Fraud-r1: A multi-round benchmark for assessing the robustness of llm against augmented fraud and phishing inducements. *arXiv preprint arXiv:2502.12904*.
- Zhengyuan Yang, Linjie Li, Kevin Lin, Jianfeng Wang, Chung-Ching Lin, Zicheng Liu, and Lijuan Wang. 2023. The dawn of lmms: Preliminary explorations with gpt-4v (ision). *arXiv preprint arXiv:2309.17421*, 9(1):1.
- Qinghao Ye, Haiyang Xu, Jiabo Ye, Ming Yan, Anwen Hu, Haowei Liu, Qi Qian, Ji Zhang, and Fei Huang. 2024. mplug-owl2: Revolutionizing multimodal large language model with modality collaboration. In *Proceedings of the IEEE/CVF conference on computer vision and pattern recognition*, pages 13040–13051.
- Shukang Yin, Chaoyou Fu, Sirui Zhao, Ke Li, Xing Sun, Tong Xu, and Enhong Chen. 2023. A survey on multimodal large language models. *arXiv preprint arXiv:2306.13549*.
- Shukang Yin, Chaoyou Fu, Sirui Zhao, Tong Xu, Hao Wang, Dianbo Sui, Yunhang Shen, Ke Li, Xing Sun, and Enhong Chen. 2024. Woodpecker: Hallucination correction for multimodal large language models. *Science China Information Sciences*, 67(12):220105.
- Qifan Yu, Juncheng Li, Longhui Wei, Liang Pang, Wentao Ye, Bosheng Qin, Siliang Tang, Qi Tian, and Yueting Zhuang. 2023. Hallucidoctor: Mitigating hallucinatory toxicity in visual instruction data. *arXiv preprint arXiv:2311.13614*.
- Hang Zhang, Xin Li, and Lidong Bing. 2023. Video-llama: An instruction-tuned audio-visual language model for video understanding. *arXiv preprint arXiv:2306.02858*.
- Lin Zhang, Lijie Hu, and Di Wang. 2025. Mechanistic unveiling of transformer circuits: Self-influence as a key to model reasoning. *arXiv preprint arXiv:2502.09022*.
- Ruiyang Zhang, Hu Zhang, and Zhedong Zheng. 2024a. V1-uncertainty: Detecting hallucination in large vision-language model via uncertainty estimation. *arXiv preprint arXiv:2411.11919*.
- Zhuoran Zhang, Yongxiang Li, Zijian Kan, Keyuan Cheng, Lijie Hu, and Di Wang. 2024b. Locate-then-edit for multi-hop factual recall under knowledge editing. *arXiv preprint arXiv:2410.06331*.
- Zhiyuan Zhao, Bin Wang, Linke Ouyang, Xiaoyi Dong, Jiaqi Wang, and Conghui He. 2023a. Beyond hallucinations: Enhancing lvlms through hallucination-aware direct preference optimization. *arXiv preprint arXiv:2311.16839*.
- Zhiyuan Zhao, Bin Wang, Linke Ouyang, Xiaoyi Dong, Jiaqi Wang, and Conghui He. 2023b. Beyond hallucinations: Enhancing lvlms through hallucination-aware direct preference optimization. *arXiv preprint arXiv:2311.16839*.
- Lanyun Zhu, Deyi Ji, Tianrun Chen, Peng Xu, Jieping Ye, and Jun Liu. 2024. Ibd: Alleviating hallucinations in large vision-language models via image-biased decoding. *arXiv preprint arXiv:2402.18476*.

A More Experimental Details

We present more experimental details and results in this section.

A.1 Image Preprocessing

The extracted images are preprocessed to conform to the input specifications of the Qwen2-VL model. This preprocessing stage typically involves several key steps. First, images are resized to a standardized dimension to ensure uniformity in input size, which is crucial for maintaining consistency in model performance. Second, pixel values are normalized to a specific range, usually between 0 and 1 or using z-score normalization, to optimize the model’s convergence and accuracy. Additionally, other necessary transformations such as color space conversion, data augmentation techniques (e.g., rotation, flipping), and noise reduction may be applied as needed to enhance the quality and diversity of the input data.

A.2 Caption Generation

The preprocessed images are fed into the Qwen2-VL model to generate textual captions. During this process, each image is individually processed by the model, which leverages its vision and language components to produce a coherent and contextually appropriate caption. The model’s output is recorded for subsequent analysis, ensuring that the generated captions are both accurate and representative of the visual content.

A.3 Co-occurrence Score Calculation

For each generated caption, a Co-occurrence Score is computed to evaluate the co-occurrence patterns of objects and behaviors within the text. This score quantifies how frequently and in what manner different objects and behaviors appear together in the captions. Unlike traditional object-object co-occurrence metrics, the calculation here is adapted to focus on the relationships between objects and behaviors, as well as among behaviors themselves. This adjustment allows for a more nuanced understanding of how well the model captures the interactions and contextual relationships within the images, providing valuable insights into the model’s performance in representing real-world scenarios accurately.

Video-MME. We ensure that each group contains a diverse set of videos from different domains

Table 3: Model Performance Comparison.

Model	Recall	Precision	F1	Correlation
GPT-4V	0.120	0.180	0.132	0.23
Gemini	0.165	0.179	0.146	0.35
Video-LLaMA-2	0.197	0.067	0.125	0.19
Chat-UniVi	0.127	0.184	0.172	0.27
LLaVA-Video	0.112	0.134	0.106	0.41
MiniGPT4	0.135	0.145	0.115	0.45
mPLUG-Owl-v3	0.106	0.113	0.069	0.17
InstructBLIP	0.133	0.125	0.127	0.36

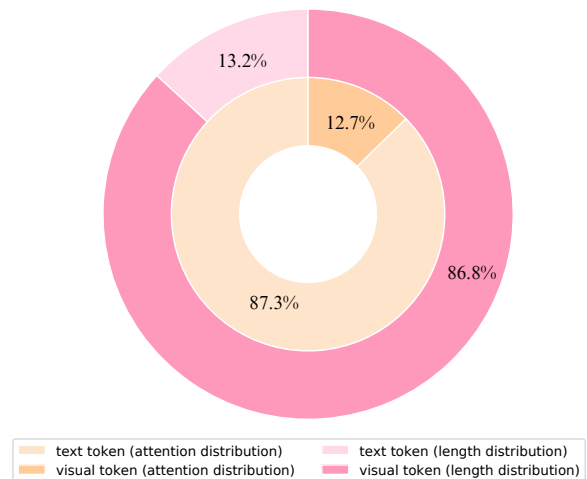


Figure 7: Attention distribution.

and sub-domains to maintain the representativeness of the dataset.

For each video in the dataset, we utilize the provided question-answer pairs to prompt the models and generate responses. The process begins with question generation, where a set of questions covering various aspects of video understanding, such as object recognition, behavior analysis, and scene comprehension, is created based on the Video-MME dataset’s question-answer pairs. Next, in the model inference stage, each video is input into the selected MLLMs, which are then asked to answer these generated questions, producing natural language responses. The generated responses are subsequently compared against the ground-truth answers from the dataset. Here, we employ a combination of exact match and semantic similarity metrics to assess the correctness of the model’s response. If the model’s response contains objects or behaviors not present in the video or the standard answers, it is flagged as a hallucination, which we further categorize into object hallucinations and behavior hallucinations.

Table 4: Behavior Hallucination Evaluation Results.

Method	Qwen-2.5VL _{behavior}			LLaVA-ov _{behavior}			LLaVA-Video _{behavior}		
	BEACH_S ↓	BEACH_I ↓	mAP ↑	BEACH_S ↓	BEACH_I ↓	mAP ↑	BEACH_S ↓	BEACH_I ↓	mAP ↑
Mementos									
DECO	49.56	91.53	0.09	54.75	69.21	0.26	57.48	68.44	0.25
VCD	46.79	63.74	0.29	49.14	66.75	0.28	51.60	69.71	0.29
OPERA	41.99	62.33	0.28	58.26	74.66	0.24	61.21	72.49	0.27
Ours	38.78	59.76	0.29	45.72	64.25	0.31	50.67	63.08	0.31
SSID									
DECO	45.05	82.73	0.18	51.44	65.42	0.28	54.01	66.83	0.26
VCD	37.67	59.15	0.33	46.62	63.74	0.29	50.35	59.91	0.30
OPERA	40.07	65.69	0.28	54.42	70.98	0.28	57.14	73.43	0.24
Ours	36.62	57.84	0.33	43.48	62.45	0.30	45.18	57.36	0.33
Visual Storytelling									
DECO	39.58	71.07	0.25	50.19	74.24	0.25	52.69	75.26	0.22
VCD	40.33	73.89	0.20	45.05	63.47	0.28	47.30	64.28	0.30
OPERA	30.79	62.14	0.31	53.40	68.44	0.27	56.06	61.71	0.31
Ours	27.12	57.42	0.33	41.90	58.89	0.30	44.00	58.84	0.33
Visual VWP									
DECO	61.86	78.55	0.21	49.43	74.96	0.25	52.30	71.91	0.25
VCD	34.47	64.54	0.27	45.05	63.47	0.29	47.66	69.97	0.27
OPERA	33.54	67.98	0.24	53.40	65.59	0.27	56.48	61.97	0.28
Ours	29.62	60.90	0.29	40.82	56.80	0.32	43.38	58.44	0.32

Table 5: VideoMME Example Data.

Video ID	Duration	Type	Subtitle Content	Question	Options	Answer
001	1 min	Edu	Hi guys, I'm going to show you how to prepare a ...	Person's clothing color?	A. Black B. Gray C. Green D. Brown	C
002	2 min	Doc	Exploring ancient ruins in the jungle...	Main subject?	A. Modern city B. Ancient ruins C. Jungle animals D. Local cuisine	B
003	3 min	Tut	Starting by gathering materials...	First step?	A. Clean workspace B. Gather materials C. Turn on machine D. Put on gloves	B

A.4 Datasets

Mementos. The Mementos dataset is a comprehensive benchmark designed to evaluate the sequential image reasoning abilities of Multimodal Large Language Models (MLLMs). We sample 5000 sequence images from the Mementos (Wang et al., 2024c), using the image captioning objective to caption methods with both Qwen2.5-vl and LLaVA-ov.

SSID. SSID (Lastname, 2025) comprises 17,365 video frames organized into 3,473 chronological 5-image sequences, each paired with four human-written, 5-sentence stories (13,892 total) to benchmark expressive and coherent visual storytelling models.

VWP. VWP (Hong et al., 2023) comprises nearly 2,000 curated sequences of movie shots,

each containing 5–10 images selected to form coherent, character-focused visual narratives.

Visual Storytelling. Visual Storytelling (Huang et al., 2016) comprises 210,819 unique Flickr photos organized into 50,000 five-image sequences (albums of 10–50 images captured within a 48-hour span), each annotated by Amazon Mechanical Turk workers with a coherent five-sentence story (one sentence per image) to benchmark sequential vision-to-language narrative generation models.

A.5 Metrics

The metrics we used, such as Recall, Precision, and F1 Score, were used to measure the models' understanding of image sequences. Additionally, for hallucination detection, we use the Mean Av-

erage Precision (mAP) metric and CHAIR metric [Rohrbach et al. \(2018\)](#). In addition to this, we are the first to propose Behavior Evaluation Assessment for Caption Hallucination (BEACH), a metric used to assess behavioral hallucinations.

$$\text{BEACH}_I = \frac{|\{\text{hallucinated behaviors}\}|}{|\{\text{all annotated behaviors}\}|},$$

$$\text{BEACH}_S = \frac{|\{\text{captions with hallucinated behaviors}\}|}{|\{\text{all captions}\}|}$$

A.6 Baselines

Deco. DeCo ([Wang et al., 2024a](#)), a dynamic correction decoding method for reducing hallucinations in MLLMs. DeCo adaptively selects preceding layers and integrates knowledge into the final layer to adjust output logits, effectively mitigating hallucinations.

VCD. VCD ([Leng et al., 2023](#)) is a method designed to mitigate object hallucinations in large vision-language models (LVLMs) by leveraging contrastive decoding.

OPERA. OPERA ([Huang et al., 2024](#)) is a novel decoding method that introduces an Over-trust Penalty and a Retrospection-Allocation strategy to mitigate hallucinations without additional data, knowledge, or training.

A.7 Ablation Study

Ablation on Correction Strength α_{base} . We compare fixed α_{base} [1,6] versus dynamic α_{base} strategies (same value range) using Mementos’s test set containing 100 manually annotated over-correction and under-correction cases. We vary the α_{base} and measure changes in the rate of detected hallucinatory behavior, rate of hallucinatory behavior, and rate of elimination of hallucinatory behavior. Figure 5 shows that as the α_{base} increases, our method is getting better at removing the hallucination, but by looking at the actual model output and analyzing it, we found that the model output becomes uninformative and useless, when the α_{base} is too high.

Ablation on Temporal Window Coefficient γ . We investigate how the window coefficient γ [0.2,0.8] affects behavior complexity adaptation. For each value of γ , we analyze correction success rates, and we monitor the reduction in hallucination across various layers designated for editing. We extract latent embeddings for the text embedding and exclude the parameters that lead to

a decrease in correctly identified behavior. Pearson correlation quantifies the coefficient-accuracy relationship. When γ takes on an appropriate value—typically in the range of 0.4 to 0.6—and the targeted layer lies in the middle-to-late stages of the network, our method achieves a favorable balance between eliminating hallucinations and preserving the validity of the model’s outputs. If γ becomes too large, the removal accuracy (as shown in the figure) deteriorates; likewise, a layer-wise analysis reveals that applying the removal at either the earliest or the very last layers yields inferior results compared to intervening in the mid-to-late layers.